

# A New Bismuth Magnesium Vanadate with Reduced Vanadium: $\text{BiMg}_{2.5}\text{V}_{18.5}\text{O}_{38}$

S. Uma and A. W. Sleight

*Department of Chemistry, Oregon State University, Corvallis, Oregon 97331*

Received July 17, 2001; in revised form November 5, 2001; accepted November 16, 2001

A new oxide containing Bi, Mg, and V has been prepared, and its structure was determined from single-crystal X-ray diffraction data. The space group is  $R\bar{3}$  with hexagonal cell dimensions of  $a = 10.1985(9)$  and  $c = 20.4875(14)$  Å. The formula may be written as  $\text{BiMg}_2(\text{MgV})\text{V}_{18}\text{O}_{38}$  to indicate that one crystallographic site is occupied by a 1:1 mixture of Mg and V. The vanadium on that site appears to be in an oxidation state of 2. Thus, the average oxidation state of vanadium on the other three vanadium sites would be 3.72+. The site occupied exclusively by magnesium is in tetrahedral coordination to oxygen. All sites occupied by vanadium are octahedrally coordinated by oxygen. The low electrical resistivity of this compound suggests itinerant electron behavior. © 2002 Elsevier Science (USA)

## INTRODUCTION

For reported complex oxides containing bismuth and vanadium, the oxidation states are usually 3 for Bi and 5 for V. However, there are several compounds reported in the Bi/V/O system where the oxidation state of V is  $< 5$ . Galy and co-workers (1, 2) have shown the existence of Aurivillius phases of the type  $(\text{Bi}_2\text{O}_2)_2\text{V}_{2x}\text{O}_{4x+2}$  ( $x = 1-4$ ). The most reduced phase reported in the Bi/V/O system is  $\text{Bi}_{1.7}\text{V}_8\text{O}_{16}$  with the hollandite structure and an average V oxidation state of 3.36 (3). Although  $\text{Bi}_2\text{V}_3\text{O}_9$  has also been reported (4, 5), its existence has been questioned by Abraham and Mentre (3).

We have prepared many new oxides containing bismuth, vanadium, and a divalent cation (6–10), but always the oxidation state of V was 5. We have now extended this study to search for phases containing Bi(III), M(II) cations, and V in an oxidation state  $< 5$ .

## SYNTHESIS

Reactants were  $\text{Bi}_2\text{O}_3$  (Cerac, 99.99%),  $\text{V}_2\text{O}_5$  (Johnson Matthey, 99.9%), and  $\text{MgO}$  (Aldrich, 99 + %). Our  $\text{V}_2\text{O}_5$  was prepared by reducing  $\text{V}_2\text{O}_5$  under  $\text{H}_2$  at 875°C for 12 h.

A mixture of reactants to give the composition 2:1:6:16 Bi:Mg:V:O was intimately mixed and placed in an alumina boat, which in turn was placed in a silica ampoule sealed under vacuum. This sample was heated at 600°C for 12 h and then at 1000°C for 24 h, followed by slow cooling at a rate of 5°C/h. The product was a mixture of yellow  $\text{BiVO}_4$  powder and irregular platelike black crystals. Microprobe analysis and structure determination of the black crystals gave a formula of  $\text{BiMg}_{2.5}\text{V}_{12.5}\text{V}_6\text{O}_{38}$ . A polycrystalline sample of this composition was then prepared using an appropriate mixture of reactants in a sealed silica ampoule at 950°C. An X-ray powder diffraction pattern obtained on a Siemens D5000 diffractometer using  $\text{Cu } K\alpha$  radiation indicated a single-phase product with the pattern expected based on the single-crystal structure determination. The  $\text{BiMg}_{2.5}\text{V}_{12.5}\text{V}_6\text{O}_{38}$  formula was further confirmed by thermogravimetric analysis of the powdered sample upon heating in air when heated to 700°C. The resulting weight gain was consistent with this formula (observed, 10.72%; calculated, 10.77%).

## STRUCTURE DETERMINATION

A crystal was mounted on a glass fiber for collection of single-crystal X-ray diffraction data. Details of the data collection are given in Table 1. The data were collected using the  $\omega-2\theta$  scan technique at a scan width of  $\Delta\omega = (1.6 + 0.3 \tan \theta)$ . The intensities of three standard reflections measured every 150 reflections throughout data collection exhibited no significant fluctuations.

The initial data processing and an absorption correction by  $\phi$  scan to the full data set were applied using the programs from the TEXSAN crystallographic software package (11). The structure was then solved by direct methods and refined using SHELXS97 incorporated in the WINGX suite (12, 13). The Bi and V positions found by direct methods were refined by least squares. The oxygen and Mg atoms were then located in a difference Fourier map. The difference Fourier map also indicated that Bi was actually displaced off the 3b site in a disordered manner. Splitting Bi

**TABLE 1**  
Crystal Data and Intensity Collection for  $\text{BiMg}_{2.5}\text{V}_{18.5}\text{O}_{38}$

Color, habit	Black, irregular plate
Size ( $\text{mm}^3$ )	$0.13 \times 0.06 \times 0.04$
Diffractometer	Rigaku AFC6R
Radiation	$\text{MoK}\alpha$ ( $\lambda = 0.71069 \text{ \AA}$ )
Monochromator	Graphite
Temperature	$23^\circ\text{C}$
Maximum $2\theta$ (deg)	55
Data collected	$-14 \leq h \leq 14, 0 \leq k \leq 14,$ $0 \leq l \leq 28$
Scan type	$\omega$ - $2\theta$
Scan speed	8
Absorption correction	Psi-scan
Transmission factors, range	1.00–0.62
Crystal system	Rhombohedral
Space group	$R\bar{3}$ (No. 148)
Unit cell dimensions ( $\text{\AA}$ )	10.1985(9), 20.4875(14) <sup>a</sup>
Volume ( $\text{\AA}^3$ )	1845.4(3)
Z	3
Formula weight	5500.38
Calculated density ( $\text{g/cm}^3$ )	4.913
Absorption coefficient ( $\text{mm}^{-1}$ )	14.005
No. of reflections collected in primitive setting	4721
Total reflections for rhombohedral setting	1541
No. of unique reflections	951, $R_{\text{int}} = 10.64$
No. of observed reflections ( $I > 2\sigma(I)$ )	785
Refinement method	Full-matrix least-squares on $F^2$
No. of parameters refined	101
Goodness of fit on $F^2$	0.937
Final $R$ indices ( $I > 2\sigma(I)$ )	$R = 4.26\%$ , $wR2 = 11.77\%$
$R$ indices (all data)	$R = 6.04\%$ , $wR2 = 12.96\%$
Extinction coefficient	0.0047(5)
Largest difference peak and hole	$1.422 \text{ e \AA}^{-3}$ (0.63 $\text{\AA}$ from Bi1) and $-1.3 \text{ e \AA}^{-3}$ (0.76 $\text{\AA}$ from Bi1)

<sup>a</sup>Lattice parameters obtained from the powder X-ray diffraction.

**TABLE 2**  
Positional Parameters and  $U_{\text{eq}}$  for  $\text{BiMg}_{2.5}\text{V}_{18.5}\text{O}_{38}$

Atom	Site	x	y	z	$U_{\text{eq}}^a$ ( $\text{\AA}^2$ )
Bi <sup>b</sup>	18f	0.7012(7)	0.3625(16)	−0.1425(1)	0.028(1)
Mg	6c	$\frac{2}{3}$	$\frac{1}{3}$	0.1412(2)	0.005(1)
V1	18f	0.3063(1)	0.0751(1)	0.1012(1)	0.007(1)
V2	18f	0.6173(1)	0.1425(1)	−0.0004(1)	0.007(1)
V3 <sup>c</sup>	3a	0	0	0	0.009(1)
Mg2 <sup>c</sup>	3a	0	0	0	0.009(1)
V4	18f	0.0833(1)	−0.2430(1)	0.1107(1)	0.014(1)
O1	18f	0.4372(4)	0.0327(4)	0.0515(2)	0.006(1)
O2	18f	0.3657(4)	0.2633(4)	0.0581(2)	0.007(1)
O3	18f	0.5042(4)	−0.2065(4)	0.0560(2)	0.008(1)
O4	18f	0.4646(4)	0.1849(4)	0.1699(2)	0.007(7)
O5	18f	0.1338(4)	−0.0529(4)	0.0622(2)	0.008(1)
O6	18f	0.2644(4)	−0.1033(4)	0.1606(2)	0.006(1)
O7	6c	$\frac{2}{3}$	$\frac{1}{3}$	0.0458(3)	0.004(1)

<sup>a</sup>Equivalent isotropic  $U$  defined as one-third of the trace of the orthogonalized  $U_{ij}$  tensor.

<sup>b</sup>Bi in the 3b sites are split and placed in 18f with the occupancy of  $\frac{1}{6}$ .

<sup>c</sup>V3 and Mg2 occupying the 3a site and the occupancies are refined to 0.54756(2) and 0.45246(2), respectively.

into six using the general position reduced  $R$  from 25.1 to 8.9% and gave more reasonable thermal parameters for Bi. An unusual feature of the structure at this point was a high thermal parameter for the V atom placed at the origin and an unusual thermal ellipsoid for O5 that bonds to this atom at the origin. This suggested partial substitution of V by Mg at this site. Refinement of occupancies at the origin site leads to 55% V and 45% Mg. The other three V sites were tested for possible Mg occupancy, but all refined to 100% V. Final

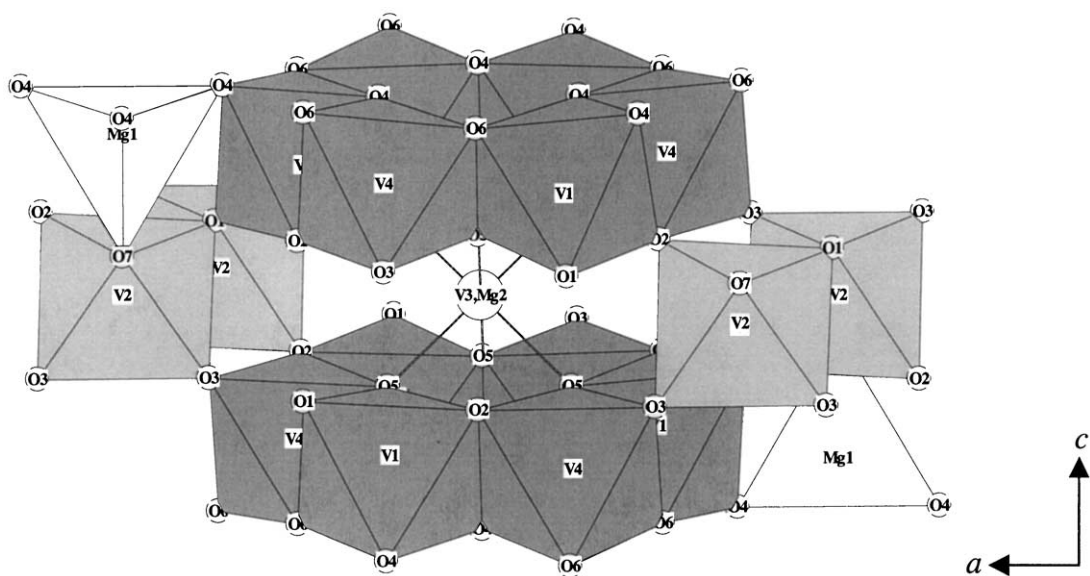


**FIG. 1.** The crystal structure of  $\text{BiMg}_{2.5}\text{V}_{18.5}\text{O}_{38}$  showing the edge and corner sharing of different  $\text{VO}_6$  octahedra and  $\text{MgO}_4$  tetrahedra along  $\sim 010$ .

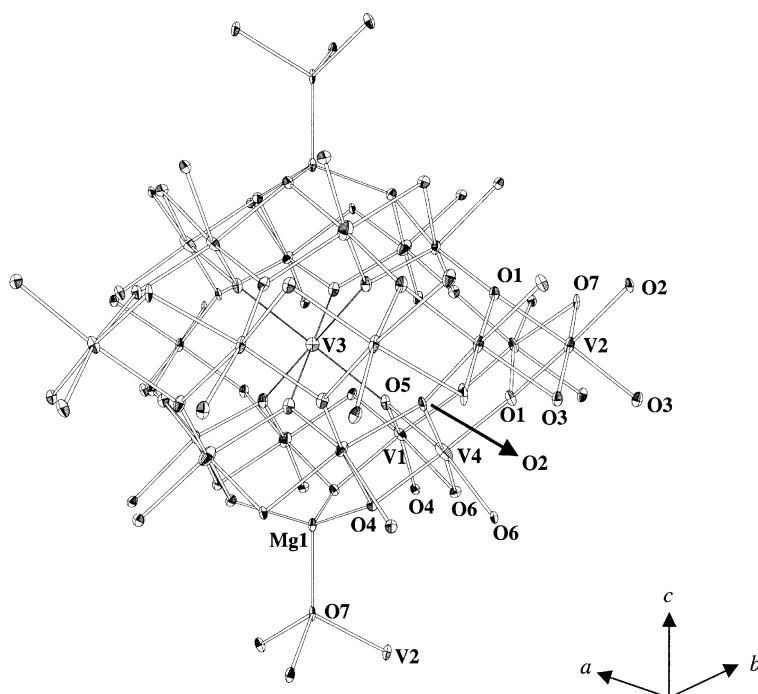


FIG. 2. Connections of various vanadium and magnesium oxygen polyhedra along 110. Atoms are drawn at 90% probability level.

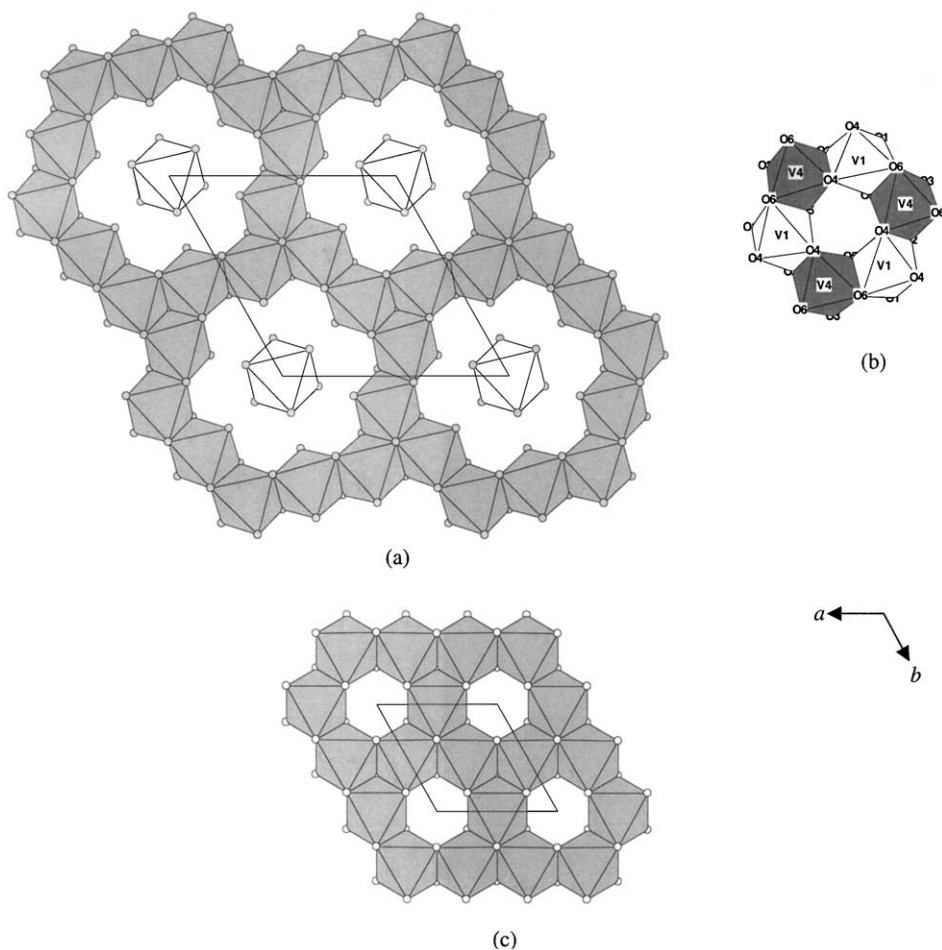


FIG. 3. (a) Edge sharing of V2 octahedra (shaded) around a (V3, Mg2) octahedron. (b) V1 and V4 octahedra sharing edges. (c) Edge-sharing kagomé-type network in  $AV_6O_{11}$  ( $A = \text{Na, Sr}$ ).

**TABLE 3**  
**Anisotropic Displacement Parameters for  $\text{BiMg}_{2.5}\text{V}_{18.5}\text{O}_{38}$**

Atom	$U_{11}$	$U_{22}$	$U_{33}$	$U_{23}$	$U_{13}$	$U_{12}$
Bi	0.028(3)	0.031(5)	0.025(1)	0.014(2)	-0.022(1)	-0.014(2)
Mg	0.0034(8)	0.0034(8)	0.0095(14)	0.0017(4)	0	0
V1	0.0041(5)	0.0065(5)	0.0092(6)	0.0007(3)	0.0012(3)	-0.0025(3)
V2	0.0047(5)	0.0039(5)	0.0117(6)	0.0012(3)	0.0016(3)	-0.0018(3)
V3	0.009(1)	0.009(1)	0.010(2)	0.004(1)	0	0
Mg2	0.009(1)	0.009(1)	0.010(2)	0.004(1)	0	0
V4	0.0108(5)	0.0127(5)	0.0154(6)	0.0041(4)	0.0029(3)	-0.0054(3)
O1	0.005(2)	0.006(2)	0.009(2)	0.003(1)	0.000(1)	-0.001(1)
O2	0.007(2)	0.003(1)	0.009(2)	0.002(1)	0.000(1)	0.002(1)
O3	0.006(2)	0.006(2)	0.011(2)	0.003(1)	-0.003(1)	-0.001(1)
O4	0.006(2)	0.006(2)	0.007(2)	0.003(1)	0.001(1)	0.000(1)
O5	0.006(2)	0.007(2)	0.012(2)	0.004(1)	0.000(1)	-0.001(1)
O6	0.007(2)	0.003(2)	0.007(2)	0.001(1)	0.000(1)	0.001(1)
O7	0.000(1)	0.000(1)	0.012(3)	0.000(1)	0	0

$R$  values are in Table 1. The refined atomic positional and isotropic thermal parameters are in Table 2, and the anisotropic thermal parameters are in Table 3. Selected bond distances and angles are given in Table 4.

The structure of  $\text{BiMg}_{2.5}\text{V}_{18.5}\text{O}_{38}$  in polyhedral representation is shown in Fig. 1. Thermal ellipsoids of the different atoms in the unit cell are shown in Fig. 2. All three cation sites occupied 100% by V have octahedral coordination, and Mg1 is on the  $\bar{3}$  axis with tetrahedral coordination. The octahedral site occupied by a mixture of Mg and V is at an inversion center on the  $\bar{3}$  axis. The octahedra based on V1 and V4 share edges to form hexagonal rings using O1, O2, O3, O4, O5, and O6 (Fig. 3a). The octahedra based on V2 share edges to form trimers, which in turn share edges to form a hexagonal net (Fig. 3b). This net surrounds the Mg/V octahedron but forms no bonds to it. The V2 octahedra share corners with the V1 and V4 octahedra using O1, O2, and O3. The Mg/V octahedron on the  $\bar{3}$  axis shares corners with the V1 and V4 octahedra using O5 (Figs. 1 and 2). The Mg1 tetrahedron on the  $\bar{3}$  axis shares three corners with V1 and V4 octahedra using O4 and one corner with a V2 octahedron using O7. A hexagonal net of edge-shared V(III) octahedra is also found in  $\text{AV}_6\text{O}_{11}$  ( $A = \text{Sr}, \text{Na}$ ) (14) compounds, but the connectivity is different (Fig. 3c).

The V–O bond lengths based on Shannon radii (15) for vanadium and oxygen coordinations of 6 and 3 are 2.15 Å for  $\text{V}^{2+}$ , 2.00 Å for  $\text{V}^{3+}$ , 1.94 Å for  $\text{V}^{4+}$ , and 1.90 Å for  $\text{V}^{5+}$ . The observed average V–O bond distances (Table 4) are 1.945 Å for V1, 1.957 Å for V2, and 1.959 Å for V4. These distances thus suggest a vanadium oxidation state of 4 or somewhat less at these three sites. All the (V3, Mg2)–O5 distances are equal at 2.124 Å compared to an expected Mg–O distance of 2.08 Å. This suggests that the oxidation state of V at this site is close to 2. The Mg–O distances

(Table 4) in the tetrahedron average 1.943 Å, in good agreement with the Shannon radii prediction of 1.93 Å.

Bond valence sums (16) were calculated for the different atoms, and the results are given in Table 5. These suggest an oxidation state close to 4 for V1 and a somewhat lower average oxidation state for V2 and V4. The results of bond valence sum calculations for Bi are complicated by positional disorder, and such calculations for the V3/Mg2 site are complicated by occupational disorder. The bond valence sums for the oxygen atoms O1, O2, O4, and O7 agree with V1 and V2 in a 4+ state and V4 in a 3+ state, which leaves V3, the only possibility of a 4+ state. The

**TABLE 4**  
**Selected Interatomic Distances (Å) and Bond Angles (deg) for  $\text{BiMg}_{2.5}\text{V}_{18.5}\text{O}_{38}$**

Bi–O(3)	2.258(13)	V(2)–O(1)	1.925(4)
–O(3)	2.299(13)	–O(1)	1.898(4)
–O(3)	2.593(4)	–O(2)	1.893(4)
–O(6)	2.476(10)	–O(3)	2.016(4)
–O(6)	2.582(14)	–O(3)	2.018(4)
Mg–O(4) × 3	1.941(4)	–O(7)	1.990(3)
–O(7)	1.953(8)	V(3)–O(5) × 6	2.124(4)
		Mg(2)–O(5) × 6	2.124(4)
V(1)–O(1)	1.893(4)	V(4)–O(2)	1.986(4)
–O(2)	1.915(3)	–O(3)	1.911(4)
–O(4)	2.009(4)	–O(4)	1.969(4)
–O(4)	2.027(4)	–O(5)	2.004(4)
–O(5)	1.773(4)	–O(6)	1.911(4)
–O(6)	2.053(3)	–O(6)	1.975(3)
Bi1–Bi1	0.568(4)	V2–V2	2.6871(17)
Bi1–Bi1	1.044(3)	V2–V2	3.0306(15)
Bi1–Bi1	1.189(4)	V2–V2	3.0306(18)
V1–V4	2.8910(12)		
V1–V4	2.9449(13)		
V1–V4	2.9897(14)		
O(4)–Mg–O(7)	107.69(14)	O(3)–V(2)–O(3)	84.5(2)
O(4)–Mg–O(4)	111.19(13)	O(5)–(V(3) Mg(2))–O(5)	92.25(14)
O(5)–V(1)–O(4)	92.59(16)	O(5)–(V(3) Mg(2))–O(5)	180.00(16)
O(5)–V(1)–O(4)	162.17(17)	O(5)–(V(3)Mg(2))–O(5)	87.75(14)
O(5)–V(1)–O(4)	43.09(12)	O(5)–(V(3)Mg(2))–O(5)	180.0(2)
O(2)–V(1)–O(6)	169.92(15)	O(2)–V(4)–O(5)	92.46(15)
O(4)–V(1)–O(6)	80.00(14)	O(3)–V(4)–O(4)	176.60(16)
O(4)–V(1)–O(6)	92.68(15)	O(3)–V(4)–O(6)	88.90(15)
O(4)–V(1)–O(4)	77.15(16)	O(3)–V(4)–O(2)	93.68(15)
O(1)–V(2)–O(1)	90.68(16)	O(3)–V(4)–O(5)	93.77(16)
O(1)–V(2)–O(2)	93.63(15)	O(4)–V(4)–O(6)	94.45(15)
O(1)–V(2)–O(3)	93.17(15)	O(2)–V(4)–O(2)	82.93(15)
O(1)–V(2)–O(3)	168.50(15)	O(4)–V(4)–O(5)	86.15(16)
O(1)–V(2)–O(3)	86.46(15)	O(6)–V(4)–O(3)	95.93(16)
O(1)–V(2)–O(3)	96.94(16)	O(6)–V(4)–O(3)	84.60(15)
O(1)–V(2)–O(3)	95.02(15)	O(6)–V(4)–O(6)	90.62(15)
O(1)–V(2)–O(7)	174.25(18)	O(6)–V(4)–O(2)	94.16(15)
O(1)–V(2)–O(7)	90.38(15)	O(6)–V(4)–O(2)	174.30(16)
O(2)–V(2)–O(1)	93.07(16)	O(6)–V(4)–O(5)	167.87(16)
O(2)–V(2)–O(3)	173.19(15)	O(6)–V(4)–O(5)	82.29(15)
O(2)–V(2)–O(3)	95.02(15)		
O(2)–V(2)–O(7)	92.0(3)		

**TABLE 5**  
**Bond Valence Sums (BVS) for the Atoms in  $\text{BiMg}_{2.5}\text{V}_{18.5}\text{O}_{38}$**

Atom	R <sub>O</sub> (Å)	B (Å)	BVS	Atom	BVS
Mg(1)	1.693	0.37	<b>+2 2.03</b>	O(1) with V(1) V(2)	
			<b>+4 +4</b>	<b>+4 +3</b>	<b>2.163</b>
V(1)	1.743	0.37	<b>+3 3.601</b>	O(2) with V(1) V(2) V(4)	
			<b>+4 4.023</b>	<b>+4 +4 +4</b>	<b>2.026</b>
V(2)	1.743	0.37	<b>+3 3.403</b>	<b>+4 +4 +3</b>	<b>1.965</b>
	1.784	0.37	<b>+4 3.801</b>	O(4) with V(1) V(4) Mg(1)	
V(4)	1.743	0.37	<b>+3 3.360</b>	<b>+4 +4 +2</b>	<b>2.181</b>
	1.784	0.37	<b>+4 3.753</b>	<b>+4 +3 +2</b>	<b>2.117</b>
				O(7) with V(2) Mg(1)	
				<b>+4 +2</b>	<b>2.214</b>
				<b>+3 +2</b>	<b>2.034</b>

Note. Numbers in bold indicate the expected bond valence sum obtained for the formula  $\text{BiMg}_{2.5}^{2+}\text{V}_{12.5}^{4+}\text{V}_6^{3+}\text{O}_{38}$ .

formula can be written as  $\text{Bi}^{3+}\text{Mg}_{2.5}^{2+}\text{V}_{12.5}^{4+}\text{V}_6^{3+}\text{O}_{38}$ . This assumes that each crystallographic V site has an integer oxidation state.

Placing Bi at an inversion center on the  $\bar{3}$  axis in the  $3b$  special position (Fig. 4a) would give a regular 12-fold coordination with all Bi–O distances being 2.76 Å. Such a regular centrosymmetric environment is not expected for this lone pair cation. Furthermore, bond valence calculations show that it would be severely underbonded (2.002 instead of 3.0) in such an environment. In fact, Bi is displaced 0.59 Å off the inversion center in a disordered manner (Fig. 4b). Such disordered displacements of Bi(III) from a high-symmetry site have been observed in several other oxides, for example,  $\text{Bi}_{12.7}\text{Co}_{0.3}\text{O}_{19.35}$  (17),  $\text{Bi}_9\text{V}_2\text{ClO}_{18}$  and  $\text{Bi}_{6.67}(\text{PO}_4)\text{O}_4$  (18, 19), and  $\text{Bi}_2\text{Ti}_2\text{O}_7$  (20). This displacement of Bi from the inversion center gives shorter Bi–O distances in a reasonable range of 2.26 to 2.59 Å (Table 4).

## ELECTRICAL PROPERTIES

The single crystals were too small for electrical resistivity measurements. Therefore, a pellet was sintered at 950°C for these measurements. A 4-probe measurement from 270 to 200 K showed decreasing resistivity with increasing temperature (Fig. 5). The room-temperature resistivity is about 1.5 Ω-cm. Such low resistivity suggests the possibility of metallic behavior with the apparent activated conductivity being due to grain boundary resistance. Many of the V–V distances (Table 4) across the shared octahedral edges are in the range where metal–metal bonding is expected. One

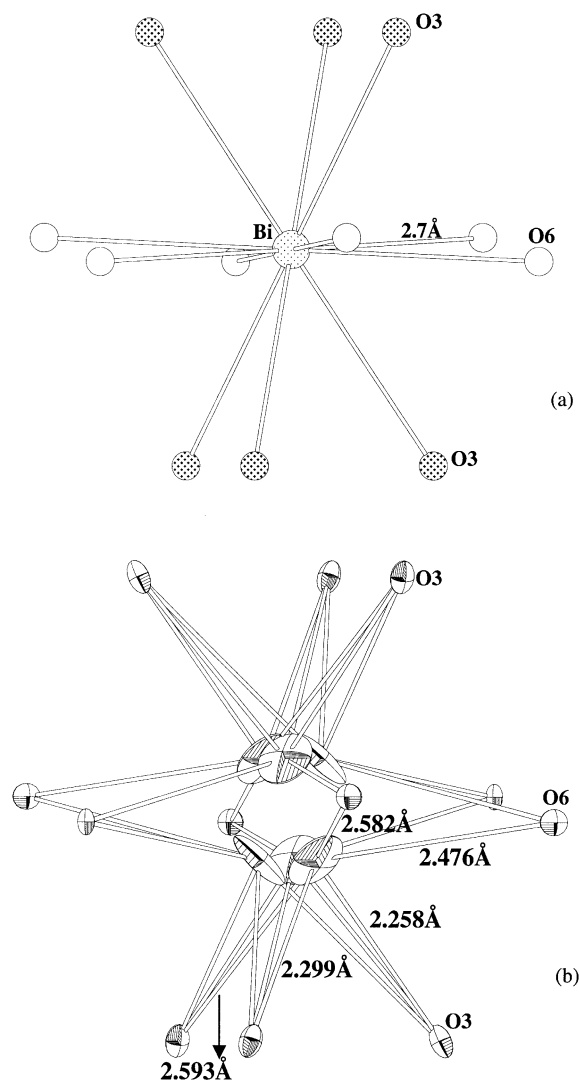


**FIG. 4.** Oxygen coordination around (a) the undistorted bismuth and (b) the split bismuth along 110. Atoms drawn at 50% probability level.

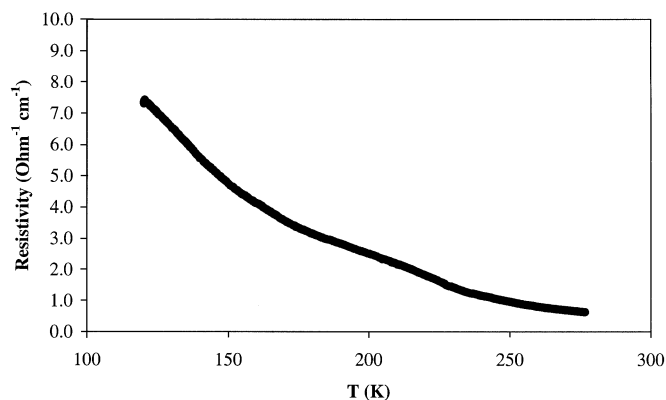


**FIG. 5.** Variation of electrical resistivity with temperature for the polycrystalline sample of  $\text{BiMg}_{2.5}\text{V}_{18.5}\text{O}_{38}$ .

would reasonably expect metal-like behavior from the metal-metal bond distances of V2–V2 (2.68–3.03 Å) and V1–V4 (2.89–2.99 Å) (Table 4). A critical evaluation of V–V separation depending upon localized and itinerant electrons has been derived based on the investigations carried out in different vanadium oxides with vanadium in different oxidation states (21,22). The critical V–V separation for vanadium oxides for an integral number of localized versus itinerant 3d electrons per cation was determined to be  $2.93 \pm 0.04$  Å (22). In our compound all short V–V distances lie in the *ab* plane. Thus, the electrical resistivity may be much higher along the *c* axis.

#### ACKNOWLEDGMENT

This work was supported by NSF Grant DMR-9802488.

#### REFERENCES

1. J. Galy, R. Enjalbert, P. Millan, and A. Castro, *C. R. Acad. Sci. Paris II* **317**, 43 (1993).
2. S. Sorokina, R. Enjalbert, P. Baules, A. Castro, and J. Galy, *J. Solid State Chem.* **125**, 54 (1996).
3. F. Abraham, and O. Mentre, *J. Solid State Chem.* **109**, 127 (1994).
4. A. Ramanan, J. Gopalakrishnan, and C. N. R. Rao, *J. Solid State Chem.* **60**, 376 (1985).
5. K. B. R. Varma, G. N. Subbanna, T. N. Guru Row, and C. N. R. Rao, *J. Mater. Res.* **5**, 2718 (1990).
6. J. Huang and A. W. Sleight, *J. Solid State Chem.* **100**, 170 (1992).
7. J. Huang and A. W. Sleight, *J. Solid State Chem.* **104**, 52 (1993).
8. I. Radosavljevic, J. S. O. Evans, and A. W. Sleight, *J. Solid State Chem.* **137**, 143 (1998).
9. I. Radosavljevic and A. W. Sleight, *J. Solid State Chem.* **149**, 143 (2000).
10. J. S. O. Evans and A. W. Sleight, *Int. J. Inorg. Mater.* **2**, 375 (2000).
11. TEXSAN, Single Crystal Structure Analysis Software, Version 5.0. Molecular Structure Corporation, The Woodlands, TX, 1989.
12. G. M. Sheldrick, Shelxs-97—A Program for Crystal Structure Refinement, release 97-2. University of Goettingen, Germany, 1997.
13. L. J. Farrugia, WinGX Ver 1.63.01, *J. Appl. Crystallogr.* **32**, 837 (1999).
14. Y. Kanke, K. Kato, E. Takayama-Muromachi, and M. Isobe, *Acta Crystallogr. C* **48**, 1376, (1992).
15. R. D. Shannon, *Acta Crystallogr. Sect. A* **32**, 751 (1976).
16. I. D. Brown and D. Altermatt, *Acta Crystallogr. B* **41**, 244 (1985).
17. T. A. Mary, R. Mackay, P. Nguyen, and A. W. Sleight, *Eur. J. Solid State Chem.* **33**, 285 (1996).
18. O. Mentre and F. Abraham, *J. Solid State Chem.* **136**, 34 (1998).
19. M. Ketatni, O. Mentre, F. Abraham, F. Kzaiber, and B. Mernari, *J. Solid State Chem.* **139**, 274 (1998).
20. I. Radosavljevic and A. W. Sleight, *J. Solid State Chem.* **136**, 63 (1998).
21. D. B. Rogers, R. J. Arnett, A. Wold, and J. G. Goodenough, *J. Phys. Chem. Solids* **24**, 347 (1963).
22. J. B. Goodenough, *Ann. Rev. Mater. Sci.* **1**, 101 (1971).